

Supporting Information to:

“Understanding Structure and Bonding of Multilayered Metal-Organic Nanostructures”

David A. Egger¹, Victor G. Ruiz², Wissam. A. Saidi³, Tomáš Bučko^{4,5}, Alexandre Tkatchenko²,
and Egbert Zojer¹

¹ Institute of Solid State Physics, Graz University of Technology, Petersgasse 16, 8010 Graz, Austria.

² Fritz-Haber-Institut der Max-Planck-Gesellschaft, Faradayweg 4-6, 14195 Berlin, Germany.

³ Department of Chemical and Petroleum Engineering, University of Pittsburgh, 1249 Benedum Hall, Pittsburgh, PA
15261, U.S.A.

⁴ Department of Physical and Theoretical Chemistry, Faculty of Natural Sciences, Comenius University, Mlynska
Dolina, SK-84215 Bratislava, Slovakia.

⁵ Slovak Academy of Sciences, Institute of Inorganic Chemistry, Dubravska cesta 9, SK-84236 Bratislava, Slovakia.

*Corresponding author: egbert.zojer@tugraz.at

Details on the Methodology and System Setup

All results reported in the main text have been obtained with the VASP code¹ and, if not otherwise stated, with an energy convergence criterion for the SCF cycle of 10^{-4} eV and a $\Delta\Phi$ convergence criterion of 10^{-2} eV. Due to the large surface unit-cell, we employed a 2x1x1 Monkhorst-Pack² k -point grid. We used a Methfessel-Paxton occupation scheme (smearing: 0.2 eV).³ The unit cell was 3D-periodically repeated, where we inserted a vacuum gap of ~ 20 Å in the z -direction that is perpendicular to the surface and, whenever necessary, used a counter-dipole correction to prevent spurious interactions. In case of Ag(111)-CuPc-PTCDA, we employed spin-polarized calculations owing to the odd number of electrons in the CuPc molecule. In this context, it is interesting that the results for vertical bonding distances in the fully optimized structure obtained in a spin-unpolarized optimization are similar (deviations < 0.05 Å). The PBE+vdW^{surf} method⁴ results in screened C_6 coefficients, vdW radii and polarizabilities, which in technical terms means that for the case of Ag(111)-PTCDA-CuPc the free-atom vdW parameters⁵ of silver are replaced by the screened ones.⁴ The geometry optimization was performed in internal coordinates using the GADGET code,⁶ where we kept the bottom two layers of Ag(111) fixed and relaxed the structure until all forces were below 0.01 eV/Å. We note that for Ag(111)-PTCDA-CuPc, GADGET resulted in a *ca.* five-time speed up compared to a damped molecular dynamics scheme.

For calculating the binding-energy curves and performing the full ionic relaxation, a CuPc molecule was placed onto four PTCDA molecules in a surface unit-cell as shown in Fig. 1b in the main text, which corresponds to the adsorption site denoted as “B” in Ref. ⁷. There, several other simultaneous adsorption sites and a very large unit cell have been observed, whose calculation is not yet computationally feasible. To test the impact of the adsorption site we also placed the CuPc molecule in the middle of the surface unit-cell and obtained similar results (deviations < 0.05 Å) for the adsorption distances.

To calculate the various binding-energy curves (*cf.*, Fig. 2 and Fig. 3 in the main text), several geometric parameters need to remain fixed:

(i) For obtaining the binding-energy curve between CuPc and Ag(111)-PTCDA (*cf.* Fig. 2 in the main text), we used the fully relaxed Ag(111)-PTCDA geometry and optimized an isolated planar CuPc layer. We then placed the CuPc layer on-top of Ag(111)-PTCDA and varied the CuPc-PTCDA distance without allowing any further relaxation; as mentioned in the main text, we report the distance between the average values of the carbon atoms inside CuPc and PTCDA in order to compare the calculated to the experimental results.

(ii) To obtain the binding-energy curves of the PTCDA single-layer and the CuPc-PTCDA double-layer to the Ag(111) substrate (*cf.*, Fig. 3 a & b in the main text), we first relaxed the Ag(111) surface, the isolated PTCDA single-layer and the isolated CuPc-PTCDA double-layer. In those relaxations, the coordinates of the bottom-two Ag(111) layers were kept fixed, the isolated organic layers were forced to remain planar during the relaxations, and the CuPc-PTCDA distance was set to be 3.22 Å (the eventually obtained average equilibrium distance in the full geometry optimization). We then varied the distance between the individually optimized Ag(111) and PTCDA and between the Ag(111) and CuPc-PTCDA sub-systems, respectively, again without further relaxations. Distances between the average values of the carbon atoms inside PTCDA and the hypothetical unrelaxed Ag(111) surface are reported in order to be consistent with the experimental procedure.

We note that the small reduction of the Ag(111)-PTCDA distance seen in experiment⁷ and in our fully relaxed structure (see main text) is not reproduced by the binding-energy curve calculations. This might arise from the fact that, as discussed above, in the binding-energy curves many geometric parameters are kept fixed making them only a rough approximation to a full geometry relaxation. Moreover, in the case of Ag(111)-PTCDA-CuPc, we find that the four PTCDA molecules in the relaxed structure are at different vertical distances (up to 0.05 Å) from the underlying Ag(111) depending on whether they are covered by the CuPc layer or not, supporting our interpretation that the CuPc layer “pushes” the PTCDA slightly down towards Ag(111). This effect cannot be entangled in the binding-energy curve, as for its calculation we assumed a flat PTCDA sheet (*vide supra*).

Discussion on the convergence of spin-polarized calculations

Obtaining the correct spin-polarized ground state (with a magnetic moment of $1\mu_B$) is rather difficult as the large number of atoms in the unit cell promotes many different minima with similar energies. For all calculations, we thus ensured that a spin-polarized ground state is obtained and checked that the magnetic moment is largely located at the copper atom and the surrounding nitrogen atoms bound to it. In case of the binding-energy curves, we performed two subsequent calculations: (i) A spin-unpolarized calculation, and (ii) a spin-polarized calculation with an initial magnetic moment of $1.5\mu_B$ for the Cu atom (for all other atoms $0\mu_B$) and the charge density from (i) as starting guess. Despite these precautions, we still experienced convergence issues when calculating the binding-energy curves, as can be seen, for example, in Fig. 3b of the main text (at $d = 2.53$ Å), where a deviation from a “smooth” curve is observed. We performed several different test calculations to improve the data points, *e.g.*, reduced the smearing for the occupation scheme, increased the convergence criterion in the SCF procedure, increased the number of k -points, made slight variations in the bonding distance, and tried several different starting configurations for the spin-polarized calculations. By those measures we could not improve the “smoothness” of the binding-energy curves. This indicates that the reported energy differences for systems of the size discussed here approach the limits of the numerical accuracy we could achieve with our approach. Nevertheless, throughout all tests described above, the general conclusions presented in the manuscript remained valid.

Details on used VASP version and PAW potentials

For the present calculations release 5.2.11 of the VASP code has been used together with the following PAW potentials:

Ag	PAW_PBE Ag 06Sep2000
C	PAW_PBE C_s 06Sep2000
H	PAW_PBE H 15Jun2001
O	PAW_PBE O_s 07Sep2000
Cu	PAW_PBE Cu 05Jan2001
N	PAW_PBE N_s 07Sep2000

Additional binding-energy curves

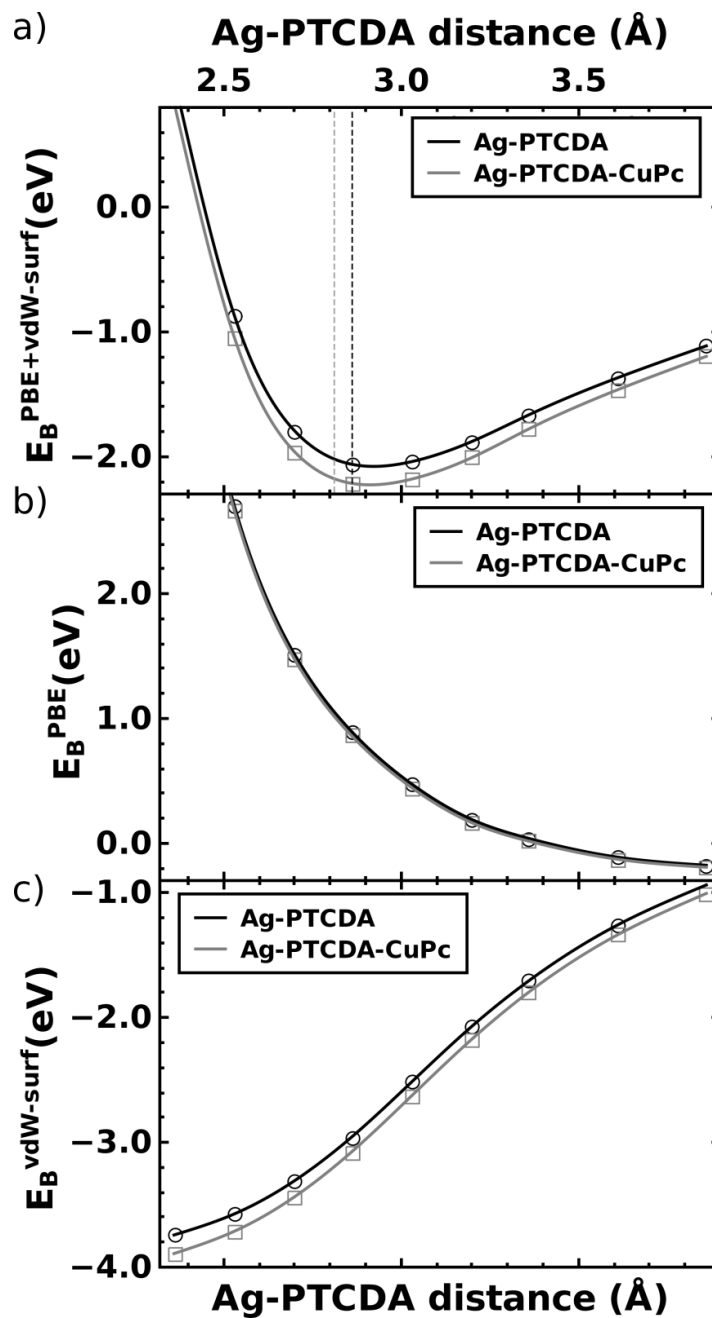


FIGURE S1: PBE+vdW^{surf} binding-energy curves (a) of a PTCDA single-layer (black) and a PTCDA-CuPc double-layer (grey), adsorbing on Ag(111) as a function of the Ag(111)-PTCDA distance; dashed vertical lines indicate the experimental binding distances⁷ for PTCDA (black) and PTCDA-CuPc (grey) on Ag(111). PBE (b) and vdW^{surf} (c) energetic contributions to the PBE+vdW^{surf} binding-energy curves in (a). These curves were used to calculate ΔE_B in Fig. 3b in the main text.

Tailing of charge density above the Ag(111) and Ag(111)-PTCDA surfaces

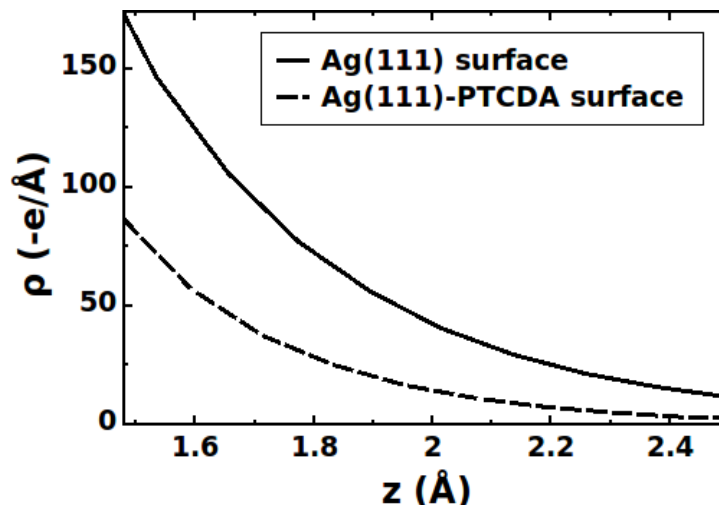


Figure S2: Plane-integrated charge density above the Ag(111) substrate relevant for PTCDA adsorption and the Ag(111)-PTCDA substrate relevant for CuPc adsorption. The reported values correspond to an integration over the area assigned to one PTCDA molecule. The origin of the horizontal axis is set in one case to the averaged positions of the atoms in the top Ag layer and in the other case to the average positions of the C atoms in the PTCDA layer. "e" refers to the (positive) elementary charge.

Impact of using soft PAW-potentials and the chosen convergence criteria

In test calculations on Ag(111)-PTCDA we experienced that replacing the "soft" PAW-potentials with "normal" ones and correspondingly increasing the plane-wave cutoff-energy by *ca.* 10 Ryd changes the vertical positions of the oxygen atoms within the PTCDA monolayer. As the interaction between Ag(111) and PTCDA could be influenced by the distance of the silver and carboxylic oxygen atoms, we have performed a non-spin-polarized optimization of Ag(111)-PTCDA-CuPc using the "normal" PAW potentials. Doing such a calculation in a spin-polarized manner appears computationally too demanding, but, as mentioned above, we found that spin-polarization only weakly affected our results. While the average positions of the carbon atoms reported in the main text change by only 0.01 Å, the average position of the carboxylic oxygens changes by 0.10 Å from 2.63 Å to 2.73 Å when replacing "soft" with "normal" PAW potentials. Interestingly, this does not impact the shift of the positions of the carboxylic oxygens induced by CuPc adsorption: Both for "soft" and "normal" potentials, their distance to the Ag(111) surface is increased by 0.05 Å.

Regarding the impact of these structural changes on the electronic structure, we find a small shift of the F-LUMO peak by 0.08 eV to lower binding energies when comparing “soft” and “normal” geometries. Most notably, however, in both sets of geometries the calculated shift of the PTCDA F-LUMO upon CuPc adsorption is only 0.01 eV. Thus, independent of the PAW-potential applied, we cannot reproduce the small shift (0.12 eV) seen in Ref. 7.

As a consequence of exchanging “soft” with “normal” PAW-potentials affecting the vertical positions of the carboxylic oxygens, the calculated work-function modification $\Delta\Phi$ also slightly changes: For both Ag(111)-PTCDA and Ag(111)-PTCDA-CuPc we observe a small lowering of $\Delta\Phi$ by 0.03 eV. As this effect is the same for both systems, it does not affect our conclusions regarding the interfacial electronic structure and the bonding induced charge transfer discussed in the main text.

As mentioned in the main text, the shear system size of Ag(111)-PTCDA-CuPc enforced us to use a rather sparse k -point grid. We calculated the effect of increasing the numbers of k -points by doubling the numbers of k -points in x - and y direction and, because of the small scale of the effects we are interested in, simultaneously decreased the energy-convergence criterion in the SCF cycle to 10^{-6} eV in a single-point calculation. As a consequence, both for Ag(111)-PTCDA and Ag(111)-PTCDA-CuPc $\Delta\Phi$ is reduced by the same, small value (0.04 eV), which again does not impact our discussion and conclusions in the main text.

Discussion of the calculated density of states (DOS)

As shown in Fig. S2, the overall shape of the valence spectra reported in Ref. 7 is reasonably well reproduced by the calculated DOS (within the well known shortcomings of Kohn-Sham orbital positions caused by self-interaction^{9,10} and by the lack of derivative discontinuity¹¹). However, similar to Ref. 8, we cannot reliably disentangle the electronic structure of the two inequivalent PTCDA molecules within the monolayer. Additionally, we do not observe a shift of the PTCDA F-LUMO peak upon CuPc adsorption, while in experiments the apparent peak maximum shifts by 0.12 eV at full CuPc coverage.⁷

Here it has to be kept in mind that the coverage we have considered is only *ca.* 40% of full coverage in experiments, for which also in Ref. 7 a much smaller shift is observed. This and the considerations involving the inequivalent PTCDA molecules described in the main manuscript lead us to conclude that capturing the subtle shift observed in the experiments for the F-LUMO and at the same time explaining why no shift of the position of the HOMO is seen would require at least the consideration of the full experimental surface unit cell and an explicit calculation of the photoionization cross-sections. Beyond that, also a much denser k -point grid and the use of harder PAW potentials would be desirable (see preceding section). All that is well beyond the scope of the present manuscript and most of it appears by no means feasible with today’s computational resources.

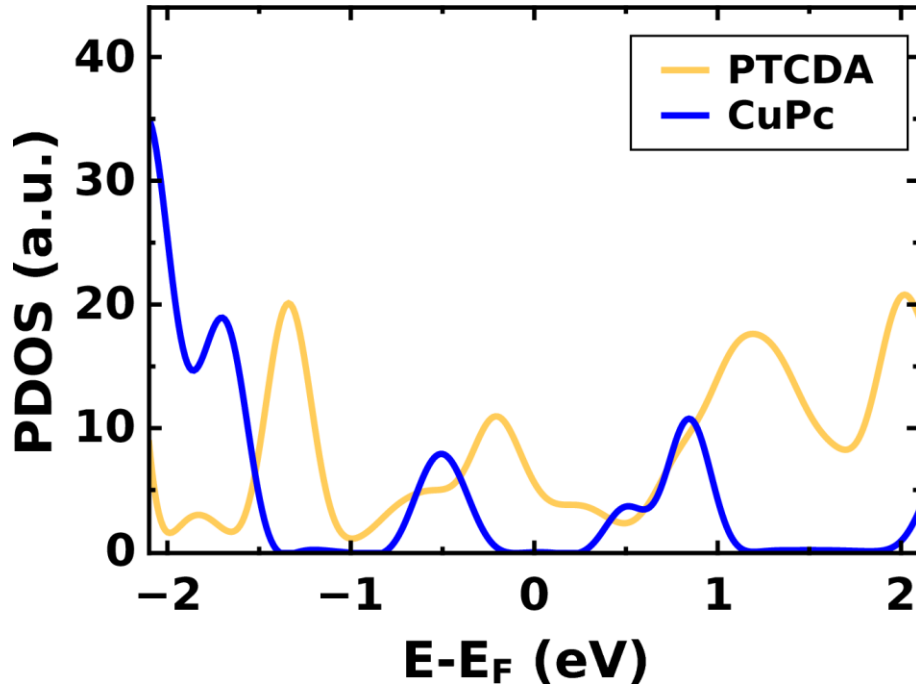


FIGURE S3: Density of states of Ag(111)-PTCDA-CuPc projected onto the PTCDA (yellow) and CuPc (blue) layers in the combined CuPc-PTCDA-Ag(111) system; the Fermi level is set to zero.

References

- (1) Kresse, G.; Furthmüller, J. *Phys. Rev. B* **1996**, *54*, 11169–11186.
- (2) Monkhorst, H. J.; Pack, J. D. *Phys. Rev. B* **1976**, *13*, 5188–5192.
- (3) Methfessel, M.; Paxton, A. T. *Phys. Rev. B* **1989**, *40*, 3616–3621.
- (4) Ruiz, V.; Liu, W.; Zojer, E.; Scheffler, M.; Tkatchenko, A. *Phys. Rev. Lett.* **2012**, *108*, 146103.
- (5) Tkatchenko, A.; Scheffler, M. *Phys. Rev. Lett.* **2009**, *102*, 073005.
- (6) Bučko, T.; Hafner, J.; Ángyán, J. G. *J. Chem. Phys.* **2005**, *122*, 124508.
- (7) Stadtmüller, B.; Sueyoshi, T.; Kichin, G.; Kröger, I.; Soubatch, S.; Temirov, R.; Tautz, F.; Kumpf, C. *Phys. Rev. Lett.* **2012**, *108*, 106103.
- (8) Rohlfing, M.; Temirov, R.; Tautz, F. *Phys. Rev. B* **2007**, *76*, 115421.
- (9) Marom, N.; Hod, O.; Scuseria, G. E.; Kronik, L. *J. Chem. Phys.* **2008**, *128*, 164107.
- (10) Körzdörfer, T.; Kümmel, S.; Marom, N.; Kronik, L. *Phys. Rev. B* **2009**, *79*, 201205.
- (11) Kümmel, S.; Kronik, L. *Rev. Mod. Phys.* **2008**, *80*, 3.